Cross-relaxation in dense ensembles of NV centers and application to magnetometry

Clément Pellet-Mary

PhD Defense

Outline

Outline

Quantum sensing and metrology

Quantum metrology:

Using quantum* properties to create more sensitive measurement protocols.

* quantum $\equiv$ discrete energy levels

Time measurement

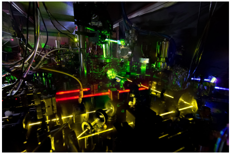

Atomic clock

Medical imaging

MRI

Magnetometry

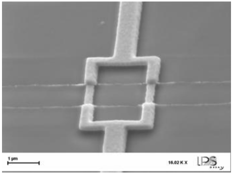

SQUIDs

Magnetometry key parameters

Magnetoencephalography

$|\vec{B}| \sim 10$ fT
$l \sim 1$ cm

Earth's magnetic field anomaly

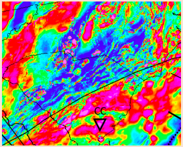

$|\vec{B}| \sim 10$ nT
$l \geq 1$ km

$|\vec{B}|$

1 T — 1 mT — 1 μT

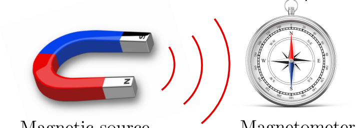

Magnetic source — Magnetometer

l_{source} — l_{working} — l_{sensing}

Optimum:

$$l_{\text{sensing}} \approx \max\{l_{\text{source}}, l_{\text{working}}\}$$

Paleomagnetism

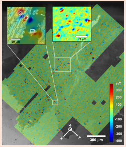

$|\vec{B}| \sim 100$ nT
$l \sim 10\ \mu$m

Surface magnetism

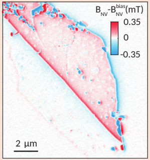

$|\vec{B}| \sim 100\ \mu$T
$l \sim 50$ nm

Sate of the art magnetometers

Mitchell, M. W., & Alvarez, S. P. *Reviews of Modern Physics*, 92(2), 021001.

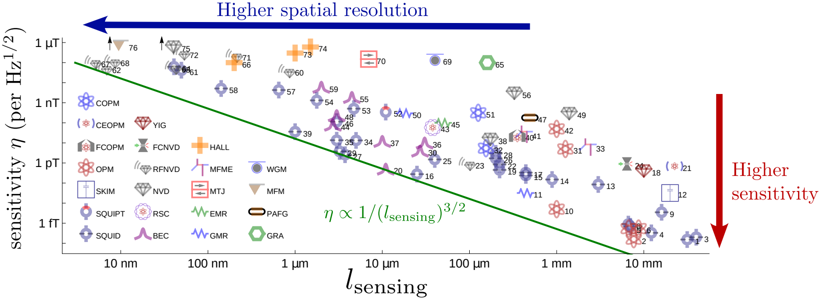

Sate of the art magnetometers

Mitchell, M. W., & Alvarez, S. P. *Reviews of Modern Physics*, 92(2), 021001.

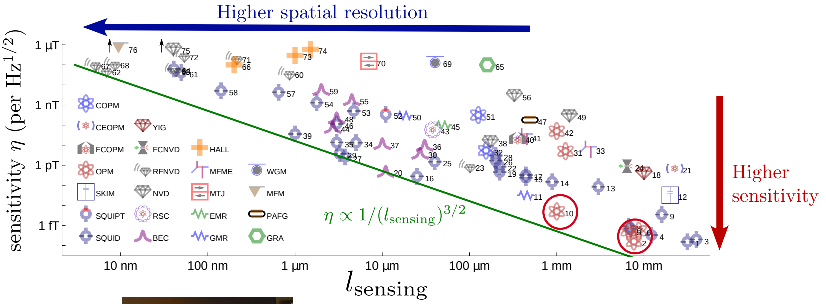

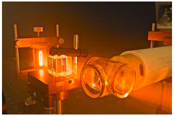

Optically pumped magnetometers (OPM)

Optically detected spin precession
of alkali vapor cell

Sate of the art magnetometers

Mitchell, M. W., & Alvarez, S. P. *Reviews of Modern Physics*, 92(2), 021001.

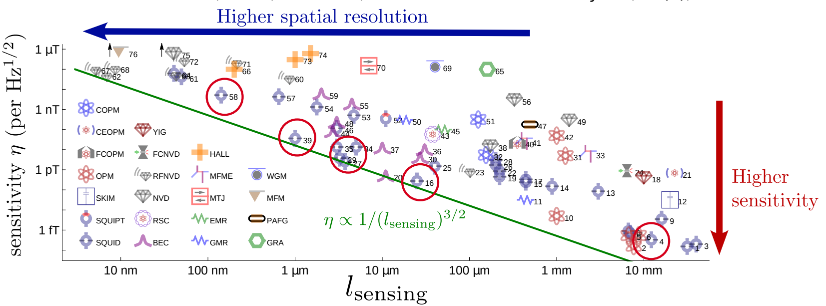

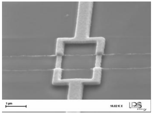

Superconducting quantum interference device (SQUID)

Magnetic field screening due to quantized magnetic flux

Sate of the art magnetometers

Mitchell, M. W., & Alvarez, S. P. *Reviews of Modern Physics*, 92(2), 021001.

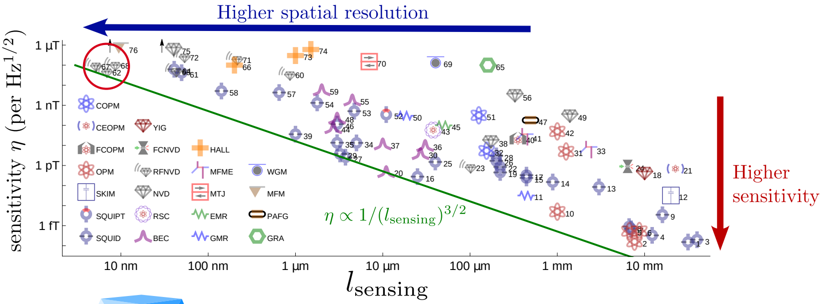

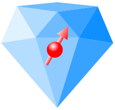

Nitrogen-Vacancy center in diamond (NV center)

Optically detetcted spin interferometry

NV center overview

Rondin, L. et al. Reports on progress in physics, 77(5), 056503.

Point-like defect in diamond

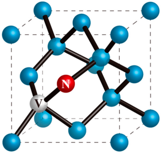

Electronic spin 1:
→ 2 spin transitions

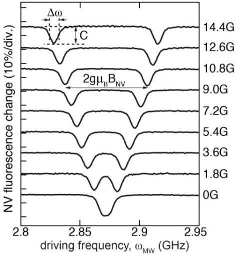

Zeeman effect:
→ linear dependance of the spin transition frequency with $\vec{B}$

- Works at room temperature
- Can be put arbitrarily close to the magnetic source (low toxicity, chemically innert)

→ Potential replacement for SQUID and OPM ?

NV center magnetometry sensitivity

Ideal (DC) sensitivity for
N independent NV centers:

$$\boxed{\eta[\mathrm{T}/\sqrt{\mathrm{Hz}}] \approx \frac{\hbar\sqrt{\Delta\nu}}{\mathrm{g}\mu_{\mathrm{B}}\mathrm{C}\sqrt{\mathrm{N}}}}$$

- $\hbar$: Planck constant
- μ_B : Bohr magneton
- g : NV electron Landé factor

} Constants

- C : Spin readout contrast } Experimental parameters

- N : Number of NV centers
- $\Delta\nu = \frac{1}{T_2^*}$: Spectral linewidth

} Sample parameters

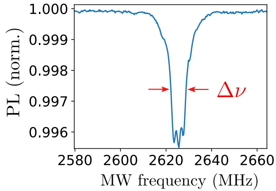

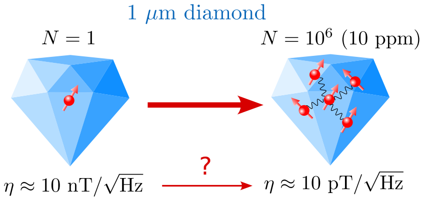

NV center magnetometry: the interaction limit

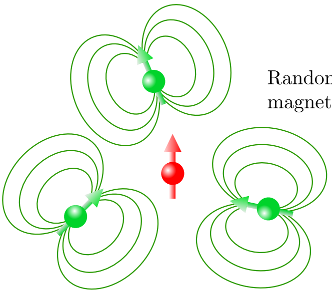

Random local magnetic noise

$= \mathrm{NV}$ $= \mathrm{N}_s$ $\frac{[\mathrm{NV}]}{[\mathrm{N_s}]} \approx 10\%$

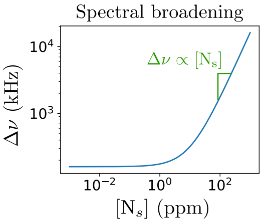

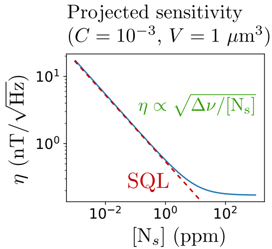

Going beyond the "Interaction limit" ($[\mathrm{N}_s] > 10$ ppm):

- Decoupling interaction (Hamiltonian engineering)
- Exploiting interactions

Outline

Colored centers in diamond

Diamond crystal lattice

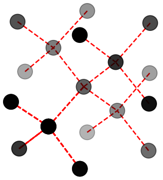

Point-like defects

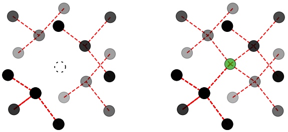

Vacancy Substitution

Colored center fluorescence

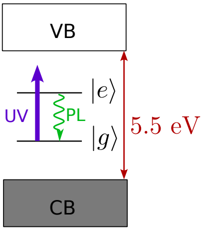

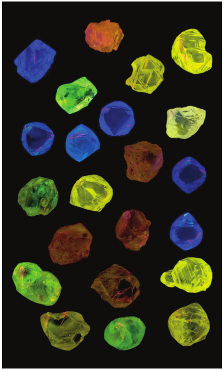

Natural diamonds fluorescence under UV light

Synthetic diamond and NV centers

NV center

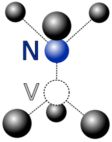

N_s (P1 center)

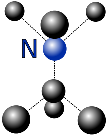

Highe Pressure High Temperature (HPHT)

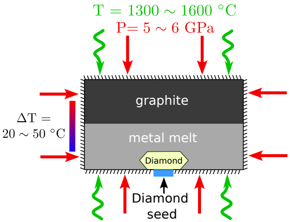

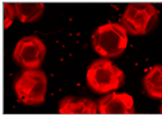

Adamas 15/150 μm
$[N_s] \approx 100$ ppm
$[NV] \approx 3$ ppm

Chemical Vapour Deposition (CVD)

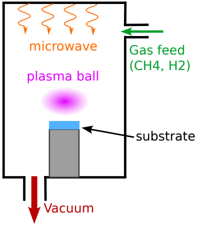

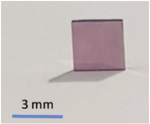

IRCP-LSPM
$[N_s] \approx 25$ ppm
$[NV] \approx 4.5$ ppm

The NV center energy levels

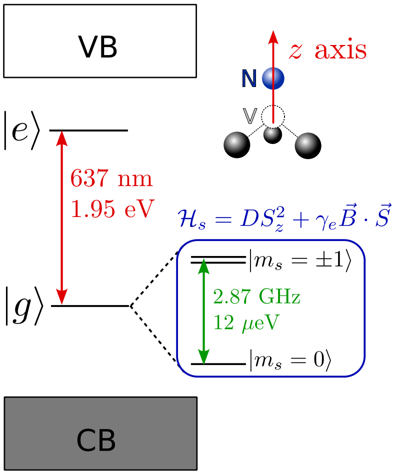

The NV center energy levels

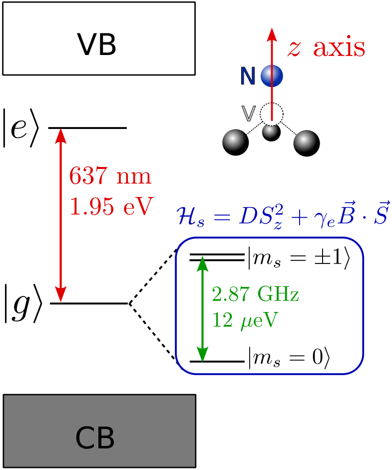

Optical pumping of the spin states

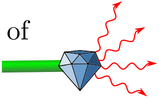

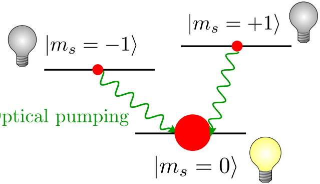

- Population accumulation in the $|0\rangle$ state
  ↳ Initialization of the spin state
- $|0\rangle$ sate brighter than $|\pm 1\rangle$ states
  ↳ Optical readout of the spin state

Experimental setup

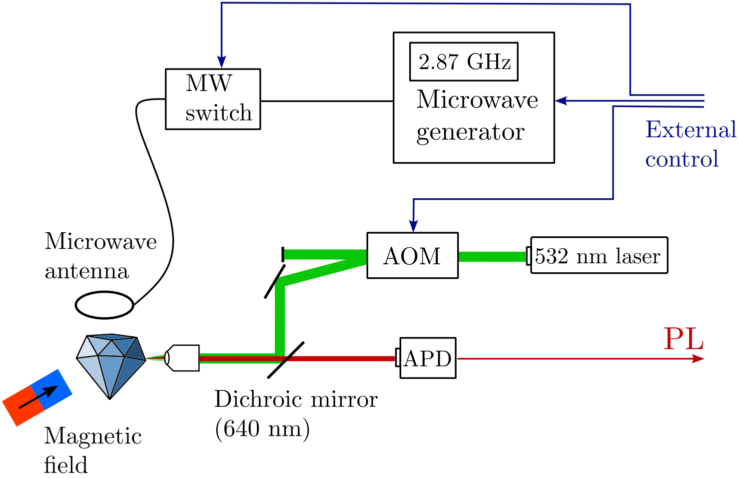

Optically detected magnetic resonance (ODMR)

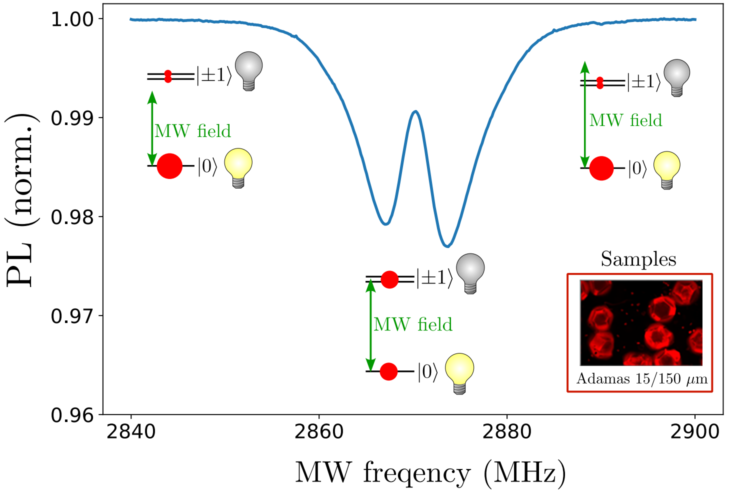

ODMR with NV ensemble

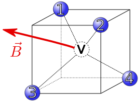

4 different projections of $\vec{B}$ over the 4 possible NV axes
$\rightarrow$ 4 classes of resonances

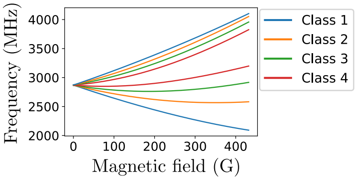

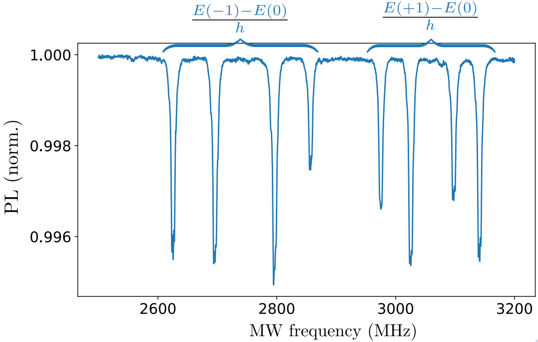

Sample

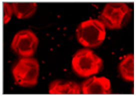

Adamas 15/150 μm

Position of the 8 lines:
$\rightarrow$ 3D reconstruction of $\vec{B}$

Transverse magnetic field effect

$$\hat{\mathcal{H}}_s = DS_z^2 + \gamma \mathbf{B} \cdot \hat{\mathbf{S}}$$

$$D = 2.87\,\mathrm{GHz},\ \gamma = 2.8\,\mathrm{MHz/G}$$

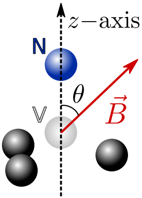

$$\begin{array}{cccc} & |-1\rangle & |0\rangle & |+1\rangle \\ \mathcal{H}_s = & \multicolumn{3}{c}{\begin{pmatrix} D - \gamma B_z & \gamma B_\perp & 0 \\ \gamma B_\perp & 0 & \gamma B_\perp \\ 0 & \gamma B_\perp & D + \gamma B_z \end{pmatrix}} \end{array}$$

When $D \gg \gamma B_\perp$:
(red circle) = Zeeman shift
(green circle) = State mixing

$$B_z = |\vec{B}| \cos\theta \quad B_\perp = |\vec{B}| \sin\theta / \sqrt{2}$$

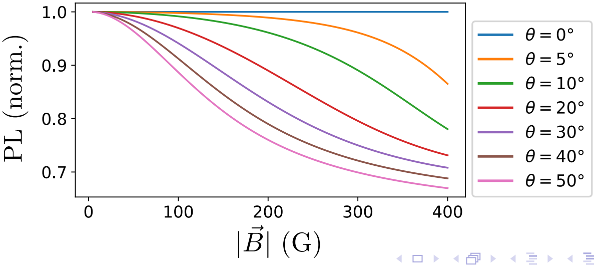

Outline

Depolarization of dense NV ensemble at low magnetic field

Transverse field

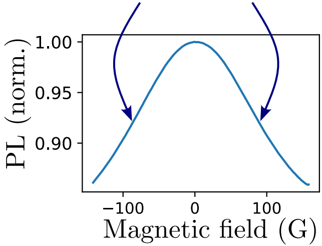

Dipole-dipole spin relaxation

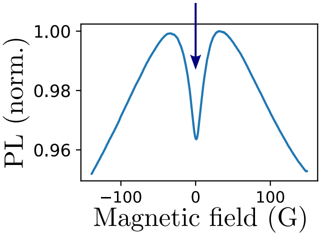

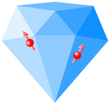

Low NV density
[NV] ≤ 100 ppb

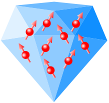

High NV density
[NV] ≥ 1 ppm

- Better understand the dipole-dipole interaction in dense NV ensembles
- Exploit the PL feature for magnetometry

LFDM experimental setup

Experimental setup

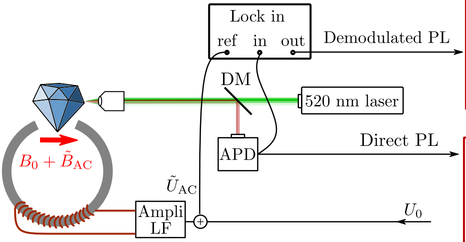

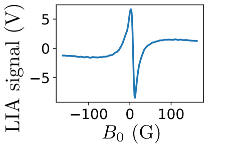

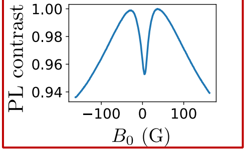

Samples

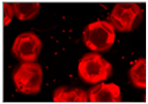

Adamas 15/150 μm

Experimental parameters

- $f_{mod} \sim 1$ kHz
- $|B_{mod}| \sim 10$ G
- $I_{las} \sim 1$ mW
- PL ~ 1 μW

Sensitivity of LFDM

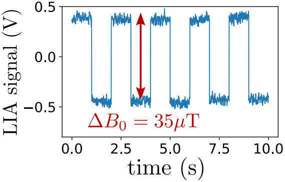

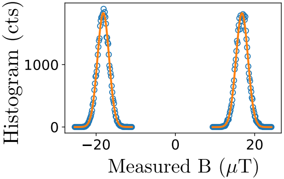

Low pass filter $\tau = 3$ ms $\quad \sqrt{\langle \delta B^2 \rangle} \approx 1.2\ \mu\mathrm{T}$

$\rightarrow$ sensitivity $\eta = \sqrt{2\tau \langle \delta B^2 \rangle} \approx 116\ \mathrm{nT}/\sqrt{\mathrm{Hz}}$

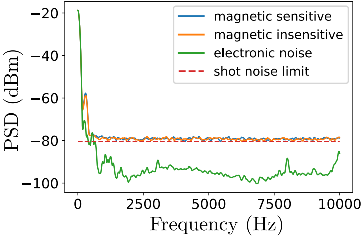

Shot noise limited for $f_{\mathrm{mod}} > 500$ Hz

Comparison with the state of the art

Sensitivity comparison

	GSLAC [1]	ODMR [2]	LFDM
η (nT/$\sqrt{\text{Hz}}$)	0.3*	0.015	116
V (μm^3)	??	$5.2 \cdot 10^6$	$3.3 \cdot 10^3$
η_v (nTμm$^{3/2}$Hz$^{-1/2}$)	??	34	6700

[1] Zheng, H.[...] Budker, D. (2020). Physical Review Applied, 13(4), 044023.
[2] Barry, J. F. [...] Walsworth, R. L (2016). PNAS, 113(49), 14133-14138.

	ODMR	GSLAC	LFDM
Microwave free	✗	✓	✓
Low magnetic field (<10 G)	✓	✗	✓
Robust to T° and B-field inhomogeneities	✗	✗	✓
Orientation free (polycrystalline, powder)	✗	✗	✓

Comparison with CW ODMR

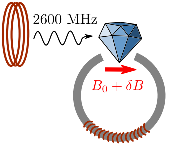

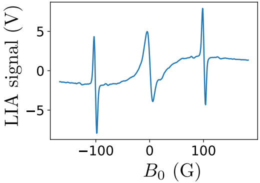

Adding a fixed microwave tone

MW slope sensitivity: $\eta \approx 40\ \mathrm{nT}/\sqrt{\mathrm{Hz}}$

B=0 sensitivity: $\eta \approx 120\ \mathrm{nT}/\sqrt{\mathrm{Hz}}$

Temporal stability

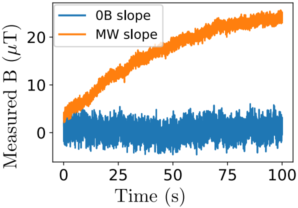

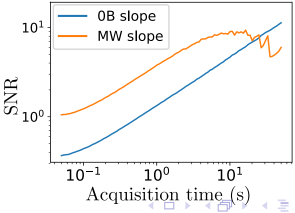

Application: wide-field magnetometry on irregular surfaces

(Commercially available 1 μm diamonds)

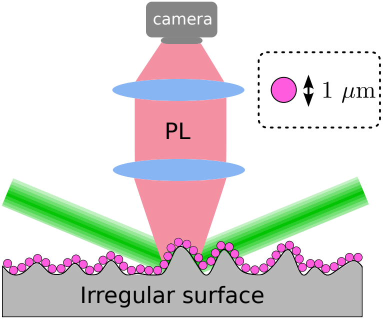

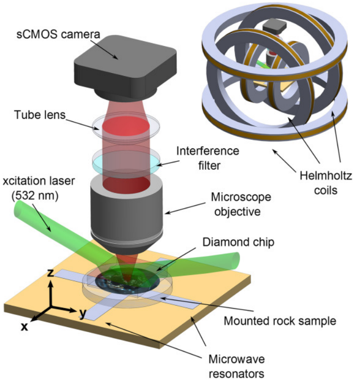

Glenn, D. R. [...] Walsworth, R. L. (2017)
Geochemistry, Geophysics, Geosystems, 18(8), 3254-3267.

Area normalized sensitivity:
$\eta_S \approx 6\ \mu\mathrm{T}\cdot\mu\mathrm{m}/\sqrt{\mathrm{Hz}}$

Area normalized sensitivity:
$\eta_S \approx 20\ \mu\mathrm{T}\cdot\mu\mathrm{m}/\sqrt{\mathrm{Hz}}$

Outline

Principle of cross-relaxation with NV centers

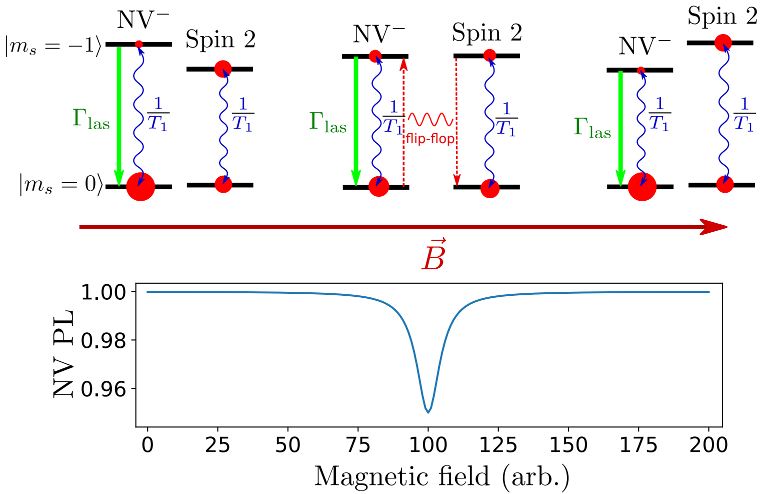

Example: Cross-relaxation between NV centers and VH^-

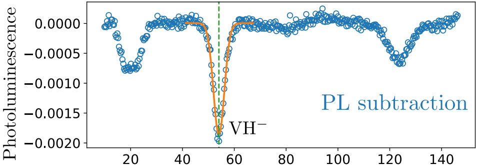

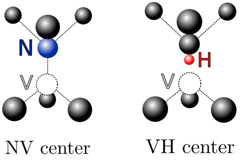

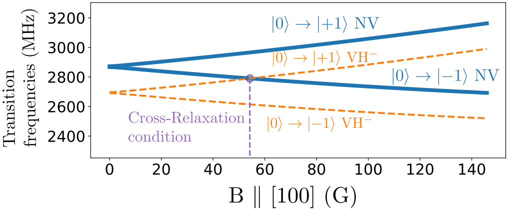

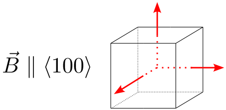

Optical detection of paramagnetic defects in diamond grown by chemical vapor deposition

C. Pellet-Mary, P. Huillery, M. Perdriat, A. Tallaire, and G. Hétet
Phys. Rev. B **103**, L100411 – Published 24 March 2021

Cross-relaxation between NV centers and NV centers

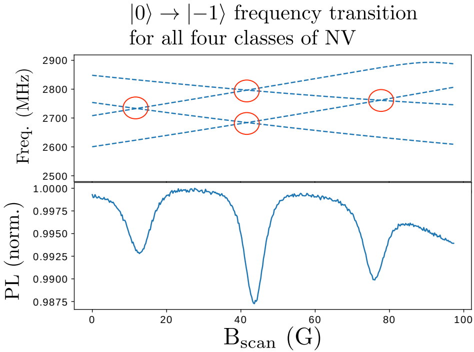

samples : Adamas 15/150 µm
fluorescent microdiamond
[N] = 100~200 PPM
[NV] ~ 3 PPM

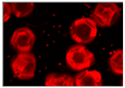

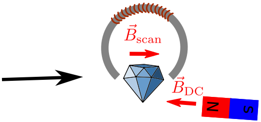

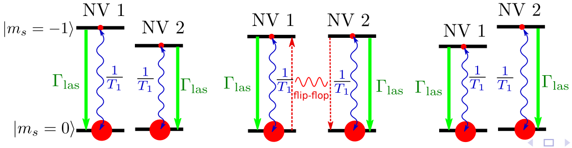

No cross-relaxation for equally polarized spins

Presentation of the fluctuator model

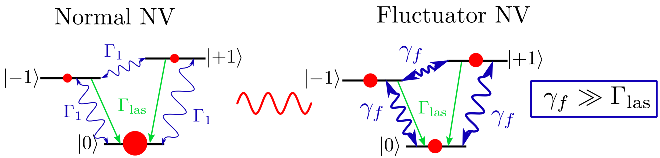

Fluctuators are NV centers with a fast intrinsic depolarization mechanism

→ Localized noise sources with the spectral response of an NV center

Precedents in:
- P-doped Si
- solid-state NMR
- FRET

Possible microscopic explanation:
- charge tunneling
- modulation of J-coupling

Up to 1/3 of all NV centers could be fluctuators

Choi, Joonhee, et al. Physical review letters 118.9 (2017): 093601.

Stretched exponential decay profile

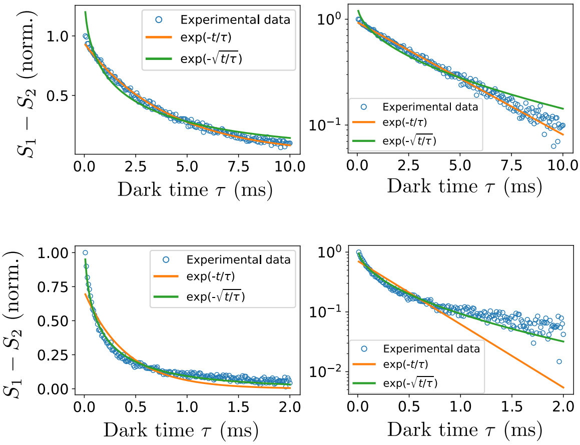

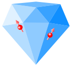

Low NV density

- Exponential profile
- $T_1 \sim 5$ ms

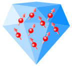

High NV density

- Stretched exp. profile
- $T_1 \sim 0.5$ ms

Zero field depolarization sources (theory)

$\boxed{\Gamma_1 = \Gamma_0^{\mathrm{th}}}$

Single class $B \neq 0$

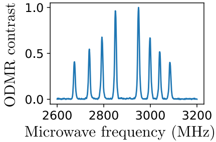

B=0

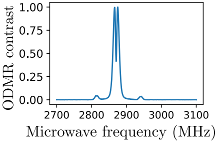

$\boxed{\Gamma_1 = 102\,\Gamma_0^{\mathrm{th}}}$

- 4-classes degeneracy
  $\Gamma_1 = \Gamma_0^{\mathrm{th}} \to 43\,\Gamma_0^{\mathrm{th}}$

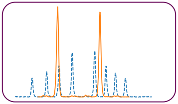

- Eigenbasis change
  $\Gamma_1 = 43\,\Gamma_0^{\mathrm{th}} \to 51\,\Gamma_0^{\mathrm{th}}$

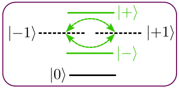

- Double flips
  $\Gamma_1 = 51\,\Gamma_0^{\mathrm{th}} \to 94\,\Gamma_0^{\mathrm{th}}$

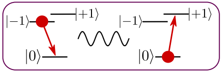

- T_2^* increase
  $\Gamma_1 = 94\,\Gamma_0^{\mathrm{th}} \to 102\,\Gamma_0^{\mathrm{th}}$

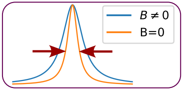

Experiment: $\vec{B}$ in arbitrary direction

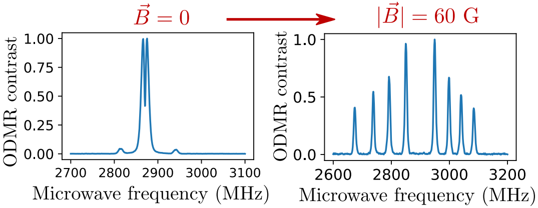

- 4-classes degeneracy
- Eigenbasis change
- Double-flips
- T_2^* change

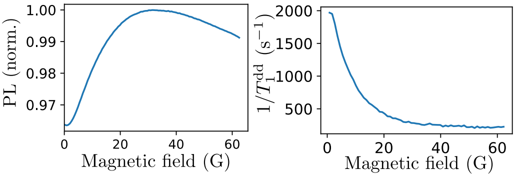

$\Gamma_1(B=0) \approx 10\ \Gamma_1(B \neq 0)$

$\sim 4\%$ PL contrast

HWHM ~ 9 G

Experiment: $\vec{B} \parallel [100]$

$\vec{B} = 0$ $\xrightarrow{\vec{B} \parallel [100]}$ $|\vec{B}| = 60$ G

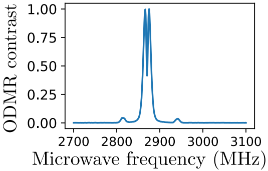

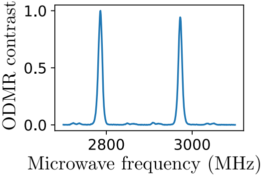

- 4-classes degeneracy
- ~~Eigenbasis change~~
- ~~Double-flips~~
- ~~T_2^* change~~

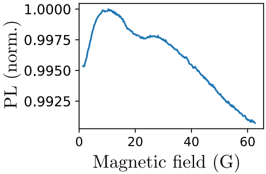

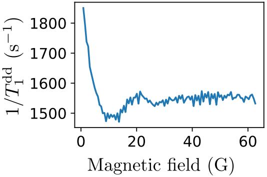

$\Gamma_1(B=0) \approx 1.2\ \Gamma_1(B \neq 0)$
$\sim 0.5\%$ PL contrast
HWHM ~ 2 G

Classes degeneracy is the dominant cause of depolarization at low magnetic field

Experiment: $\vec{B} \perp [111]$

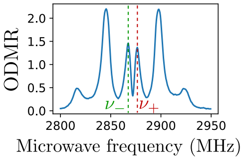

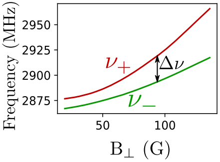

Same eigenbasis :

$$|\pm\rangle = \frac{|+1\rangle \pm |-1\rangle}{\sqrt{2}}$$

for $\vec{B} \perp [111]$ than for $\vec{B} = 0$

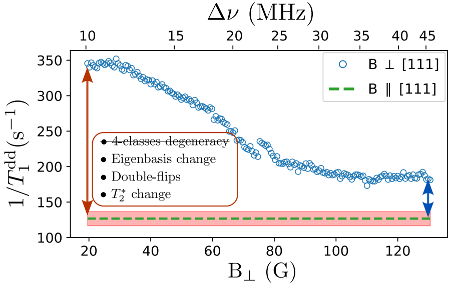

cancelling out double flips with transverse field

- ~~4-classes degeneracy~~
- Eigenbasis change
- ~~Double-flips~~
- T_2^* change

Double flips are the second dominant cause of depolarization at low magnetic field

Summary of the experimental observations

Random $\vec{B}$ direction

- 4-classes degeneracy
- Eigenbasis change
- Double-flips
- T_2^* change

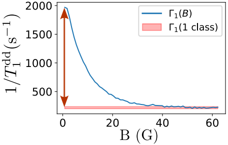

- ~~4-classes degeneracy~~
- ~~Eigenbasis change~~
- ~~Double-flips~~
- ~~T_2^* change~~

$\vec{B} \parallel [100]$

- 4-classes degeneracy
- Eigenbasis change
- Double-flips
- T_2^* change

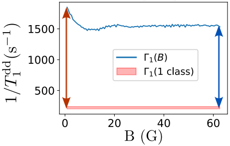

- 4-classes degeneracy
- ~~Eigenbasis change~~
- ~~Double-flips~~
- ~~T_2^* change~~

$\vec{B} \perp [111]$

- ~~4-classes degeneracy~~
- Eigenbasis change
- Double-flips
- T_2^* change

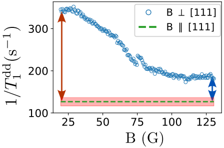

- ~~4-classes degeneracy~~
- Eigenbasis change
- ~~Double-flips~~
- T_2^* change

Angular sensitivity of LFDM

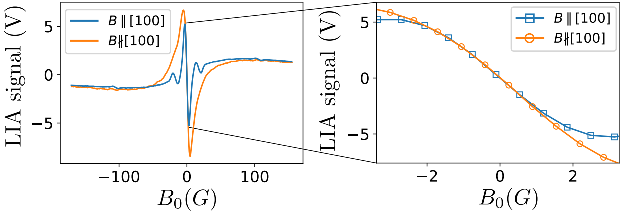

- ~~4-classes degeneracy~~
- Eigenbasis change
- Double-flips
- T_2^* change

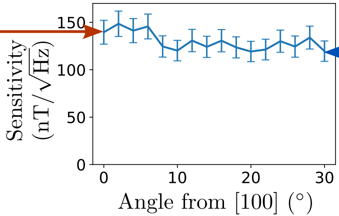

- 4-classes degeneracy
- Eigenbasis change
- Double-flips
- T_2^* change

The 4-classes degeneracy is not the limiting factor of the sensitivity

Conclusion

Acknowledgments